ACS APPLIED MATERIALS & INTERFACES

Research Article

www.acsami.org

Complexation of Bioreducible Cationic Polymers with Gold Nanoparticles for Improving Stability in Serum and Application on Nonviral Gene Delivery

Chun-Chiao Chuang and Chien-Wen Chang*

Department of Biomedical Engineering and Environmental Sciences, National Tsing Hua University, Hsinchu 30013, Taiwan

Supporting Information

ABSTRACT: Widespread applications of conventional polymeric gene carriers are greatly hampered by their inefficient transfection performance under serum-containing environment. Aiming to overcome this limitation, we propose a bioreducible polyethylenimine-gold nanocomplex system (SSPEI-Au NC), which can be prepared by a simple layer-by-layer (LBL) assembly procedure. SSPEI-Au NC contains sequentially deposited layers of bioreducible polyethylenimine (SSPEI) and poly(γ-glutamic acid) (γ-PGA) for efficient binding and delivery of plasmid DNA (pDNA). SSPEI-Au NC was characterized for various physicochemical properties, including: UV−vis spectra, TEM imaging, hydrodynamic size, and pDNA binding ability. The SSPEI-Au NC were efficiently uptaken by mammalian cells as observed using dark-field microscopy. Comparing to nondegradable PEI25k, the bioreducible SSPEI-Au NC exhibited superior transfection capability under serum-containing condition while causing lower cytotoxicity on mammalian cell lines. The effect of serum on SSPEI-Au NC dispersity was studied using UV−vis spectrometry and the results suggest that serum-assisted colloidal stability of SSPEI-Au NC contributed to its serum-resistant transfection.

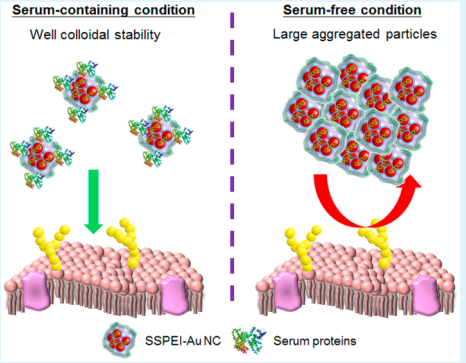

KEYWORDS: *gold nanoparticles, gene delivery, layer-by-layer assembly, serum-resistant transfection, bioreducible polyethylenimine*

INTRODUCTION

The concept of gene therapy is to treat diseases by delivering exogenous genes into cells to modulate the cellular machinery. Overexpression of designated exogenous genes may treat diseases by supplement gene products in need. On the other hand, delivery of antisense oligonucleotide or small interference RNA (siRNA) could be used to knock down genes that are vital for disease prognosis.[1,2] Nonviral-based gene delivery carriers, comparing to their viral-based counterparts, provide additional advantages, including free of mutagenesis risk, suitability of large scale production, and low immunogenicity. In recent years, cationic bioreducible polymers containing disulfide-linked backbone have emerged as a promising class of nonviral gene carrier by their excellent biological compatibility and comparable gene delivery efficiency to the nondegradable cationic gene carriers. Bioreducible polymers can be efficiently degraded by the intracellular glutathione (GSH), which promotes drug or nucleic acid release into the cytoplasm.[3−5] Despite the great potential of cationic materials on gene therapy, one of the main obstacles for their widespread applications is the inefficient gene transfection in the presence of serum.[6] The underlying mechanism might be attributed to the destabilization or aggregation of cationic polyplex or lipoplex colloids by serum components such as albumin and heparin sulfate.[7−9] To overcome this limitation, researchers have attempted various approaches such as PEGylation,[10] cationic group modifications,[11] and surface recharge.[12] Recently, it is also shown that layer-by-layer (LBL) nanoparticles possess improved stability in serum[13] and excellent in vivo stability, resulting in long circulation and low accumulation in liver.[14]

LBL assembly is a feasible approach to prepare polymer/metal nanoparticle complexes for various theranostic applications. For example, incorporation of metal nanoparticles could afford cationic polymeric gene carriers with additional theranostic applications, such as magnetic resonance imaging (MRI),[15] photothermal therapy,[16] and magnetic hyperthermia therapy.[17] Among various metal nanoparticles, gold nanoparticles have emerged as an excellent platform for drug or gene delivery, because of its bioinertness, biocompatibility, and efficient cellular uptake.[18,19] Gold nanoparticles were used as versatile scaffolds to deliver various low-molecular-weight (MW) nucleic acids such as antisense oligonucleotides,[20] microRNA, or siRNA.[21,22] Taking advantages of efficient Au−S conjugation chemistry, low MW nucleic acids can be immobilized onto gold surface under mild condition. With appropriate external stimulus, these immobilized low MW nucleic acids can be released to achieve spatial/temporal-

Received: January 24, 2015
Accepted: March 12, 2015
Published: March 12, 2015

DOI: 10.1021/acsami.5b00732
ACS Appl. Mater. Interfaces 2015, 7, 7724−7731

controlled delivery.[23] On the other hand, to deliver high MW nucleic acid such as plasmid DNA (pDNA), surface modifications of gold nanoparticles with cationic polymers are often required.[24] Meanwhile, significant cytotoxicity was observed from the gold-based gene carriers using non-degradable high MW PEI.[25]

In this study, our goal is to develop a nontoxic gene carrier capable of efficient gene transfection under serum-containing environment. To this end, we proposed a novel bioreducible SSPEI-Au NC, which can be prepared by sequentially assembling SSPEI, pDNA and poly(γ-glutamic acid) (γ-PGA) to the surface of 11-mercaptoundecanoic acid (MUA)-AuNP via a LBL assembly procedure. The material deposition conditions (MUA or SSPEI concentration effect) were studied to obtain SSPEI-Au NC with sufficient pDNA binding and delivery capability. The physicochemical properties of SSPEI-Au NC were characterized by dynamic light scattering (DLS), UV−vis spectrometry, transmission electron microscopy (TEM) and gel retardation assay, respectively. In vitro gene transfection efficiency and cell viability of SSPEI-Au NC were investigated on mammalian cell lines. The effects of serum on the colloidal stability of SSPEI-Au NC were studied using UV−vis spectroscopy.

2. EXPERIMENTAL SECTION

2.1. Reagents and Materials. 3,3′-Dithiodipropanicacid (DTPA), 1-ethyl-3-(3-(dimethylamino)propyl) carbodiimide·HCl (EDC), and *N*-hydroxysuccinimide (NHS) were obtained from Alfa Aesar (USA). Polyethylenimine, 800 Da (PEI800), and 11-mercaptoundecanoic acid (MUA) were obtained from Sigma-Aldrich (USA). $HAuCl_4$ tetrahydrate and trisodium citrate were obtained from Showa (Japan). γ-PGA (200−400 kDa) was obtained from Vedan Inc. (Taiwan). Deionized water (DI H_2O) (18.2 MΩ) was used in all experiments. pDNA encoding mOrange or firefly luciferase was amplified in *E. coli* and purified by Macherey-Nagel MidiPrep (Germany).

2.2. Synthesis of Gold Nanospheres (AuNP). Add 1 mL of $HAuCl_4$ tetrahydrate (10 mg/mL) to 99 mL of ultrapure water in a round bottle. Heat the solution under refluxing and stirring. After the solution boiled, added 2.5 mL of trisodium citrate solution (10 mg/mL) into the gold solution. The color of solution changed from light yellow to wine red. The reaction solution was cooled in the ice-bath. The as-synthesized AuNP solution was stored at 4 °C until further use.

2.3. Synthesis of Bioreducible Polymer: SSPEI. Bioreducible polymer SSPEI was synthesized according to a previously established method.[26] Briefly, DTPA:PEI800:EDC:NHS (1:1:2.5:2.5 molar ratio) was dissolved in 10 mL of DMSO and transferred to a round bottle with stirring at 30 °C for 72 h. The reaction mixture was dialyzed against DI H_2O using a dialysis membrane (MCWO 3500) for 3 days for purification.

2.4. Synthesis of SSPEI-Au NC. Adjust the pH value of AuNP solution to pH 11. Mix 0.3 mL of MUA solution (1 mg/mL) with 1 mL of AuNP solution (O.D. = 0.8). The mixed solution was reacted for 24 h at 25 °C. Unreacted MUA was removed from MUA-AuNP solution by preforming centrifugation (15,000 g/15 min) twice. Next, the MUA-AuNP pellets were resuspended in 0.9 mL of NaCl solution (10 mM). Mix 0.1 mL of SSPEI solution (30 mg/mL) with the MUA-AuNP solution and reacted at 25 °C for 48 h. Remove the free SSPEI from by SSPEI/MUA-AuNP by performing centrifugation (15,000 g/15 min) for three times. Mix SSPEI/MUA-AuNP solution with pDNA solution at various ratios by vortexing then incubated at 25 °C for 20 min. γ-PGA solution (0.01 mg/mL) was added into the solution and incubated for another 20 min before use. The amount of SSPEI in SSPEI-Au NC was determined by Thermogravimetric Analysis. The weight ratio of SSPEI in SSPEI-Au NC was calculated to be 5.63%.

2.5. Particle Size and Surface Potential Measurement of SSPEI-Au NC. SSPEI-Au NC was prepared and incubated in the following mediums, including: DMEM, DMEM+10%FBS, DMEM +25%FBS, and DMEM+50%FBS. The particle size and surface potential of SSPEI-Au NC were measured at 25 °C using the Zetasizer Nano ZS (Malvern Instruments, UK). The UV−vis spectra of the material was acquired on a UV−vis spectrophotometer (NanoDrop 2000c, Thermo Scientific, USA).

2.6. Transmission Electron Microscopy. SSPEI-Au NC was dispersed in DI H_2O and deposited onto a 300-mesh carbon-coated copper grid. Store the sample-containing copper grid at 25 °C for 4 h. Filter paper was used to wick away excess moisture. The copper grid was dried in a 65 °C oven overnight. The images were taken by TEM (HT7700, Hitachi, Japan) at 30 kV accelerating voltage.

2.7. Agarose Gel Electrophoresis. The SSPEI-Au NC/pDNA samples were freshly prepared by mixing SSPEI-Au NC with pDNA at various nitrogen/phosphate (N/P) ratios: 17, 22, 26, 30, 34, 39, and 43, then incubated at 25 °C for 20 min. Two microliters of Novel Juice (GeneDireX, USA) was added into each sample solution and mixed well. The samples were then electrophoresed in a 1% (w/v) agarose gel. Electrophoresis was carried out at a voltage of 100 V for 20 min in 1× TAE (Tris-acetate-EDTA). Finally, the results were recorded at UV light wavelength of 306 nm by a UV illuminator (UV2020−2, Top Bio Co., Taiwan).

2.8. Cellular Uptake of SSPEI-Au NC/pDNA. The intracellular uptake of SSPEI-Au NC/pDNA was observed using a dark field microscopy. MCF-7 cells were seeded over glass coverslips in a 24 well plate at the density of 5−7 × 10^4 cells/well at 37 °C overnight. The cells were incubated with SSPEI-Au NC/pDNA for 4 h at 37 °C. The cells were fixed with 4% paraformaldehyde at 25 °C for 30 min. The cells on coverslip were mounted with slides using VectaMount mounting medium (Vetor Laboratories, USA). The prepared samples were observed using a dark field microscopy (IX71, Olympus, Japan).

2.9. Cytotoxicity of SSPEI-Au NC/pDNA. HEK293T cells were seeded into a 24-well plate at the density of 5−7 × 10^4 cells/well and incubated at 37 °C for 24 h. The cells were washed by PBS once and added with the following mediums: DMEM, DMEM+10% FBS, DMEM+25% FBS, and DMEM+50% FBS. SSPEI AuNC/pDNA prepared at various N/P ratios (43, 65 and 86) were added to cells and incubated at 37 °C/5% CO_2 for 4 h. The cells were washed by PBS then incubated in 10% FBS/DMEM for another 24 and 48 h. The cells were washed with PBS then incubated with DMEM+10% FBS containing 10% (v/v) alamarBlue dye for 4 h. The absorbance at wavelength of 570 and 600 nm were detected using a microplate reader (Infinite M200 PRO, TECAN, Austria). Cells without receiving materials treatment were used as the control group, representing 100% cell viability.

2.10. Transfection Efficiency of SSPEI-Au NC/pDNA. HEK293T or MCF-7 cells were seeded in 24-well plates at the density of 5−7 × 10^4 cells/well and incubated at 37 °C/5% CO_2 for 24 h. The cells were washed by PBS once and added with the following mediums: DMEM, DMEM+10% FBS, DMEM+25% FBS, and DMEM +50% FBS. SSPEI AuNC/pDNA prepared at various N/P ratios (43, 65, and 86) were added to cells and incubated at 37 °C/5% CO_2 for 4 h. After transfection for 4 h, the cells were washed by PBS and incubated for another 72 h. The transfection efficiency of pDNA encoding mOrange (1 μg) was assessed on a fluorescence microscopy (ZEISS, Germany). The transfection efficiency of pDNA encoding firefly luciferase was quantitated using the Luciferase Assay Kit (Promega, USA). In brief, the cells were lysed in 1× lysis buffer for 10 min at 25 °C then subjected to centrifugation (15 000 g/5 min) to remove cell debris. Subsequently, the sample solutions were then mixed with equal volume of luciferase assay reagent for luminance determination on a microplate reader (Infinite M200 PRO, TECAN, Austria). The total protein concentration of the cells was measured by BCA protein assay kit (PIERCE, USA). The transfection efficiency was represented as relative luminescence unit per milligram of total protein (RLU/mg protein).

2.11. Statistics. Results of this study are presented as the mean and standard deviation of at least three independent measurements. All statistical evaluations were carried out with unpaired two-tailed

DOI: 10.1021/acsami.5b00732
ACS Appl. Mater. Interfaces 2015, 7, 7724−7731

Student's t test. p-value of less than 0.05 was considered significant ($p < 0.05$, * ; $p < 0.01$, ** ; $p < 0.001$, ***).

RESULTS AND DISCUSSION

Preparation and Characterizations of SSPEI-Au NC. SSPEI was synthesized by EDC/NHS coupling reaction as previously described.[26] Before it was used to prepare SSPEI-Au NC, gene delivery efficiency and cell cytotoxicity of the SSPEI were verified first. Efficient gene transfection by the SSPEI at various nitrogen/phosphate (N/P) ratios was observed as quantitated using FACS (Figure S1 in the Supporting Information). Comparing to nondegradable PEI25k, SSPEI displayed much lower cytotoxicity (Figure S2 in the Supporting Information), which is consistent to our previous observations.[27]

Scheme 1. Preparation of SSPEI-Au NC via Layer-by-Layer Assembly

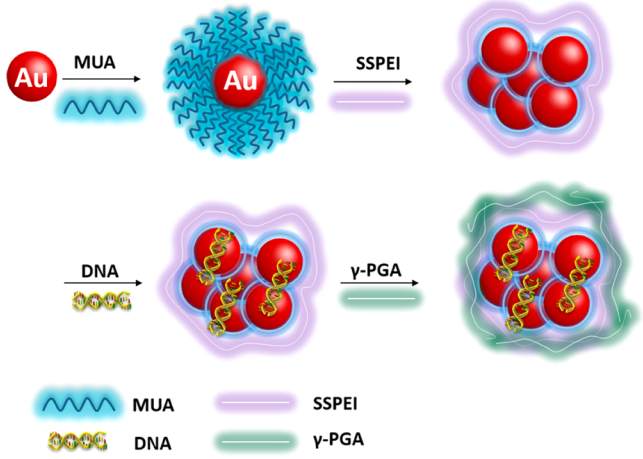

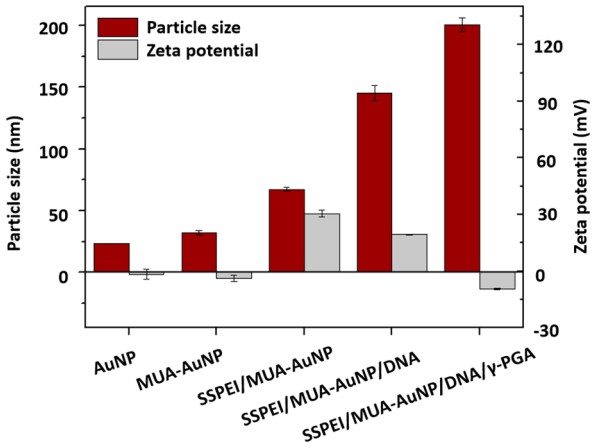

Figure 1. Evolution of particle size and surface potential of SSPEI-Au NC in the process of layer-by-layer assembly. Data represent the mean ± S.E.; $n = 3$.

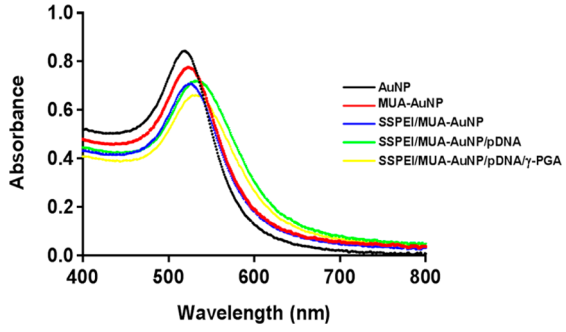

Figure 2. UV−vis spectra of SSPEI-Au NC in the process of layer-by-layer assembly.

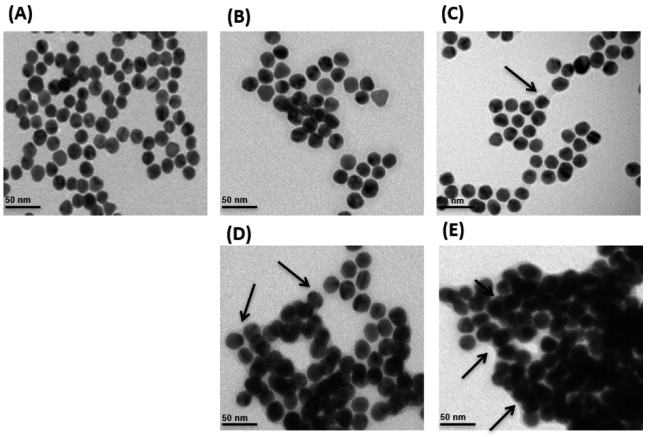

Figure 3. Transmission electron microscope (TEM) images of SSPEI-Au NC in the process of layer-by-layer assembly. (A) AuNP, (B) MUA-AuNP, (C) SSPEI/MUA-AuNP, (D) SSPEI/MUA-AuNP/pDNA, and (E) SSPEI/MUA-AuNP/pDNA/γ-PGA. The arrow indicates the SSPEI on the surface of gold nanoparticles.

LBL assembly procedure was utilized to prepare SSPEI-Au NC (Scheme 1). First, AuNP were synthesized by reducing tetrachloroauric acid with sodium citrate under reflux at 100 °C for 10 min. The as-synthesized AuNP were furthered stabilized with 11-mercaptopropanic acid (MUA) following by SSPEI adsorption via electrostatic interactions. The surface-anchored SSPEI was utilized as a cationic scaffold for pDNA loading. The effects of MUA coating concentrations or SSPEI coating concentrations on pDNA loading capability of the resultant SSPEI-Au NC were studied. With the increased concentration of MUA, surface potential of the resultant SSPEI-Au NC elevated accordingly (Figure S3A in the Supporting Information), which contributed to a stronger pDNA condensation as shown by the gel retardation assay (Figure S4A in the Supporting Information). Similarly, higher SSPEI coating concentration was found to increase surface potential and pDNA condensing ability of the SSPEI/MUA-AuNP (Figures S3B and S4B in the Supporting Information). pDNA can be fully condensed by SSPEI-Au NC at the N/P ratio of 22 (SSPEI-Au NC/pDNA).

The evolution of particle size, surface potential, and UV−vis spectra of SSPEI-Au NC in LBL assembly process was monitored. Particle size of the AuNP, MUA-AuNP, SSPEI/MUA-AuNP, SSPEI/MUA-AuNP/pDNA, and SSPEI/MUA-AuNP/pDNA/γ-PGA (Figure 1) measured using dynamic light scattering (DLS) technique were 23.5 ± 0.1 nm, 32.1 ± 2.1 nm, 67.3 ± 1.6 nm, 145.1 ± 6.0 nm, and 200.5 ± 5.3 nm, respectively. The increased size of nanocomplexes after each assembly step indicates successful materials deposition onto the surface of SSPEI-Au NC. We hypothesized that the dramatical size increase was due to the increased aggregation number of AuNP in the SSPEI-Au NC. To verify the hypothesis, we used UV−vis spectroscopy to assess the aggregation state of SSPEI-Au NC. In the process of LBL assembly, aggregation of AuNP was confirmed by observing the "Red-Shift" of gold surface

DOI: 10.1021/acsami.5b00732
ACS Appl. Mater. Interfaces 2015, 7, 7724−7731

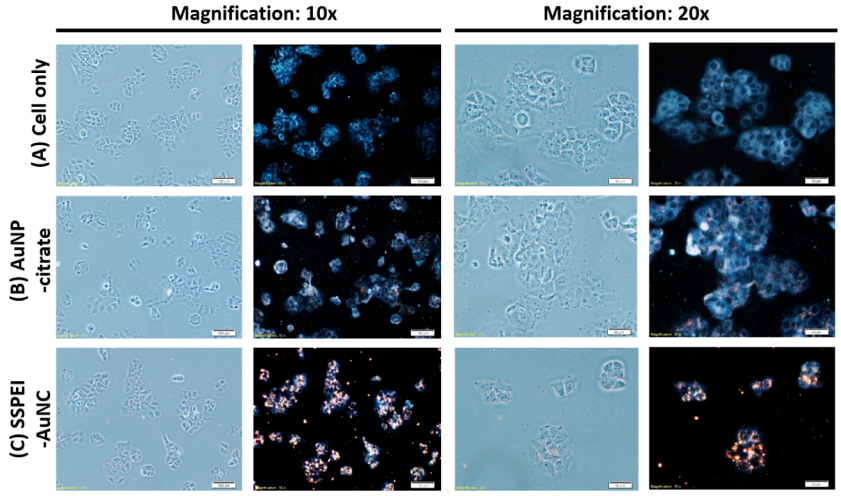

Figure 4. Cellular uptake of gold nanoparticles monitored using dark filed microscope: (A) MCF-7 cells, (B) AuNP-citrate, and (C) SSPEI-Au NC. Scale represents 100 and 50 μm under the magnification of 10× and 20×, respectively.

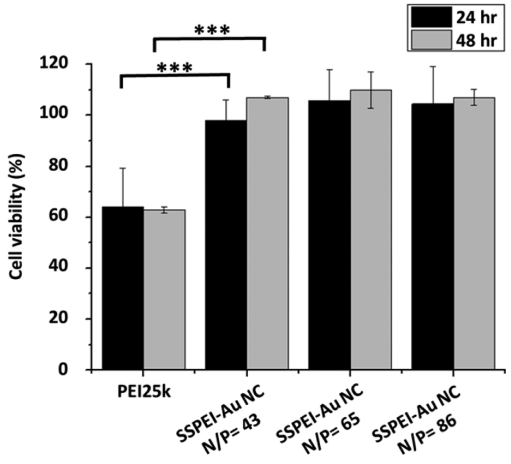

Figure 5. Cytotoxicity of SSPEI-Au NC complexes. SSPEI-Au NC/pDNA complexes prepared at various N/P ratios were added to cells for 24 and 48 h before subjecting to alamar blue assay. Data represent the mean ± S.E.; n = 3.

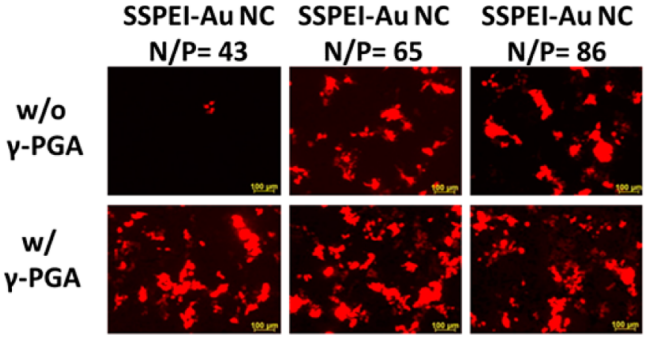

Figure 6. Effect of γ-PGA on the in vitro transfection of SSPEI-Au NC. Scale bar represents 100 μm.

plasmon resonance (SPR) after each material deposition step (Figure 2).[28] TEM imaging was used to study size and morphology of the formed SSPEI-Au NC. The results (Figure 3) show that SSPEI-Au NC contained interparticulate bridged SSPEI, pDNA, and γ-PGA, which were in good agreement with the DLS and UV−vis studies. Because the surface potential is an important factor affecting the transfection ability of nonviral gene carriers, the surface potential of the AuNP, MUA-AuNP, SSPEI/MUA-AuNP, SSPEI/MUA-AuNP/pDNA, and SSPEI/MUA-AuNP/pDNA/γ-PGA were measured to be −1.6 ± 3.9 mV, −4.8 ± 2.5 mV, +47.6 ± 2.8 mV, +30.7 ± 0.5 mV, and −13.4 ± 0.5 mV respectively (Figure 1). After each LBL assembly step, the reversal zeta potential changes indicate successful adsorption of opposite-charged polyelectrolytes onto the surface of SSPEI-Au NC. Taken together, it was certain that the SSPEI-Au NC were successfully prepared.

Cellular Uptake and Cytotoxicity of SSPEI-Au NC. Light scattering generated from the local surface plasmon resonance (LSPR) on nobel nanoparticles provides a sensitive signal for AuNP detection using dark-field microscopic techniques. After incubating the gold nanomaterials with the MCF-7 cells for 4 h, the intracellular accumulation of gold materials was observed as bright yellow and orange scattered spots using the dark field microscopic technique. When MCF-7 cancer cells were incubated with nanoparticles for 4 h, the dark-field images (Figure 4) showed that the SSPEI-Au NC (Figure 4C) had more yellow scattering spots distributed in the cytoplasm of the cells than AuNP-citrate (Figure 4B) or control cells (Figure 4A), which showed very weak scattering signal. The results clearly show that LBL surface modifications significantly enhance the cellular uptake of gold nanomaterials. Because SSPEI-Au NC is composed of biocompatible AuNP and bioreducible SSPEI, it is anticipated that the SSPEI-Au NC possess minimal cytotoxicity compared to the nondegradable gene carriers. The viability of cells incubated with the SSPEI-Au NC was studied on human HEK293T cells using alamar blue cell viability assay. The results (Figure 5) show that viability of the cells received SSPEI-Au NC maintained nearly 100% at the dose of SSPEI-Au NC/pDNA used in the transfection studies. In contrast, poor viability was observed from the cells treated with nondegradable PEI25k polymer because of its non-degradability and membrane destabilization effect.

Effect of γ-PGA on the Transfection Efficiency of SSPEI-Au NC. One of the main mechanisms underlying the efficient cellular uptake of cationic polymer-based gene carriers is via their electrostatic interactions with cell membrane-bound proteoglycans (i.e., heparin sulfate proteoglycan (HSPG)), which efficiently triggers the endocytosis process. Meanwhile, excess surface charge could hamper the gene delivery efficiency instead. Cationic polyplex recharged with anionic polymers

DOI: 10.1021/acsami.5b00732
ACS Appl. Mater. Interfaces 2015, 7, 7724−7731

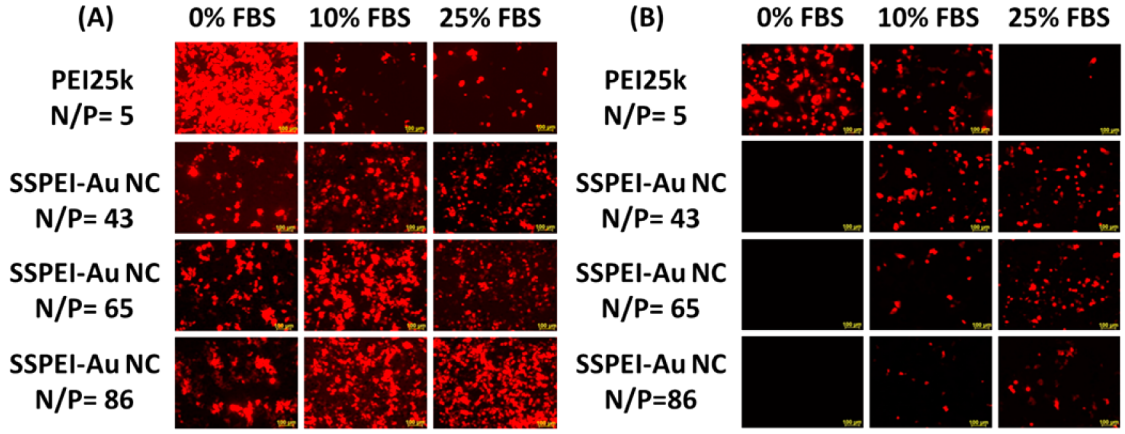

Figure 7. Effect of serum on the in vitro transfection of SSPEI-Au NC/pDNA nanocomplexes. In the presence of various serum concentrations, the designated formulations of SSPEI-Au NC/pDNA were added to transfect mammalian cells for 72 h. PEI 25 kDa was used a control. Transfection efficiency was evaluated by observing the fluorescence-positive cells (transfected cells) using a fluorescence microscopy. (A) HEK293T and (B) MCF-7 cells. Scale bar represents 100 μm.

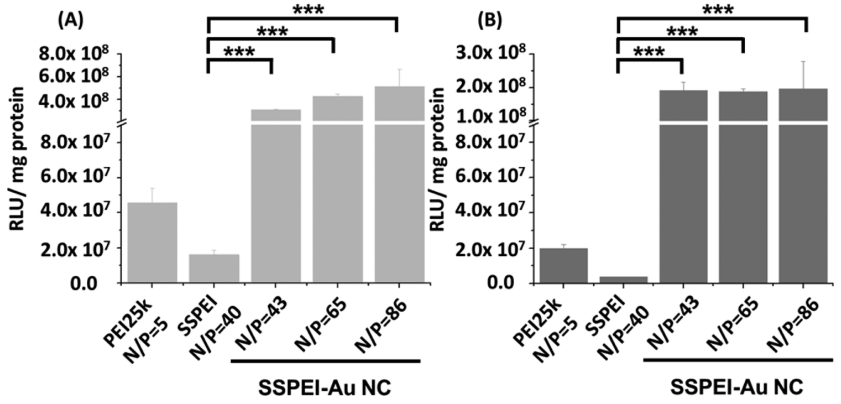

Figure 8. Quantitative measurement of the in vitro transfection of SSPEI-Au NC/pDNA nanocomplexes on HEK293T cells in the mediums with different serum concentrations: (A) 25% FBS and (B) 50% FBS. 72 h after transfection, the luminance of expressed luciferase was measured as RLU/mg protein using a plate reader. Cationic polymer PEI25k was used a control. Data represent the mean ± S.E.; n = 3.

showed improved transfection efficiency in vitro and in vivo.[12] In this study, γ-PGA was used to decorate the surface of SSPEI-Au NC to minimize the excess surface charge for better biocompatibility and gene delivery performance. γ-PGA is a water-soluble, biocompatible anionic polymer, which can be produced from fermentation techniques in large scale.[29] Under physiological conditions, the carboxylic groups (pK_a 2.9) on γ-PGA[30] are deprotonated to become negatively charged which can be readily interact with the cationic SSPEI-Au NC via electrostatic interactions. In this study, SSPEI-Au NC with or without γ-PGA coating were compared for their gene delivery efficiency. The external coating of γ-PGA coating consistently enhance the transfection efficiency of SSPEI-Au NC at the N/P ratios tested in our study (Figure 6). The uptake enhancement mechanism might be related to the γ-glutamyl transpeptidase (GGT)-mediated endocytosis of nanoparticles.[31]

Effect of Serum on SSPEI-Au NC-Mediated Transfection. Inefficient gene delivery by cationic polymeric carriers in serum-containing environment has largely limited their further in vivo gene therapy applications.[6] In this study, the effects of serum on SSPEI-Au NC-mediated transfection were investigated. Transfection efficiency of the SSPEI-Au NC formulated at various N/P ratios (N/P ratio of 43, 65, and 86) was studied on human HEK293T and MCF-7 cell lines in the presence of different amount of serum (0%, 10%, and 25% FBS). PEI25k, a nondegradable cationic polymer, was used as a control in this study. The transfection efficiency was studied by observing fluorescent gene (pmOrange) expression in the transfected cells using a fluorescence microscope. Under serum-free conditions, the transfection efficiency of PEI25k/pDNA complexes was higher than that of SSPEI-Au NC. However, the transfection efficiency of the PEI25k/pDNA complexes was significantly suppressed in the presence of serum (Figure 7A). In contrast, SSPEI-Au NC prepared at N/P ratios of 43, 65, and 86 showed higher transfection efficiency in the serum-containing mediums (10% and 25% FBS) than in serum-free medium on HEK293T cells (Figure 7A). Similar transfection performances of SSPEI-Au NC were also observed on the human breast cancer cell line (MCF-7) (Figure 7B) in serum-containing conditions. Furthermore, transfection efficiency of SSPEI-Au NC was quantitated by measuring luciferase gene expression in the transfected cells (Figure 8). On HEK293T cells, the SSPEI-Au NC maintained their transfection efficiency even under a high serum environment (25% or 50% FBS), in contrast to the decreased transfection by PEI25k under the same conditions. It has been previously suggested that binding of negatively charged biomacromolecules such as serum proteins or glycoaminoglycans (GAGs) to cationic polyplex or lipoplex may result in particle decomplexation or aggregation, which in turn contributes to inefficient gene

DOI: 10.1021/acsami.5b00732
ACS Appl. Mater. Interfaces 2015, 7, 7724−7731

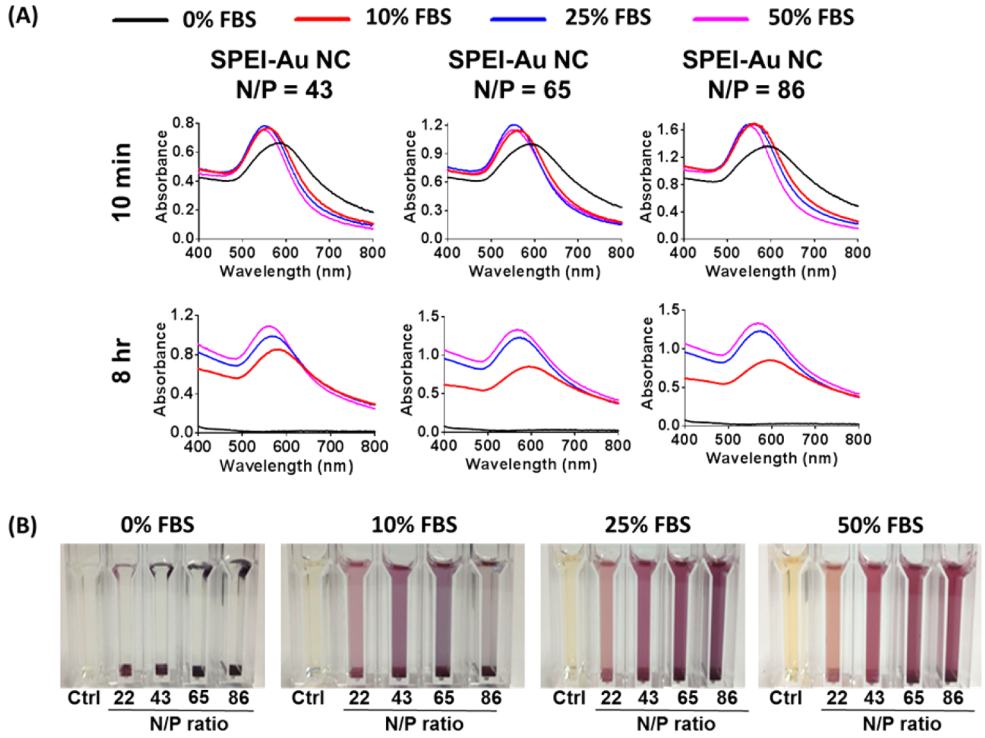

Figure 9. Colloidal stability of SSPEI-Au NC/pDNA nanocomplexes in the presence of various serum concentrations (0, 10, 25, and 50% FBS). The aggregation state of SSPEI-Au NC/pDNA nanocomplexes were studied by (A) UV−vis spectroscopy and (B) Visual check.

Scheme 2. Effect of Serum on the in Vitro Transfection of SSPEI-Au NC

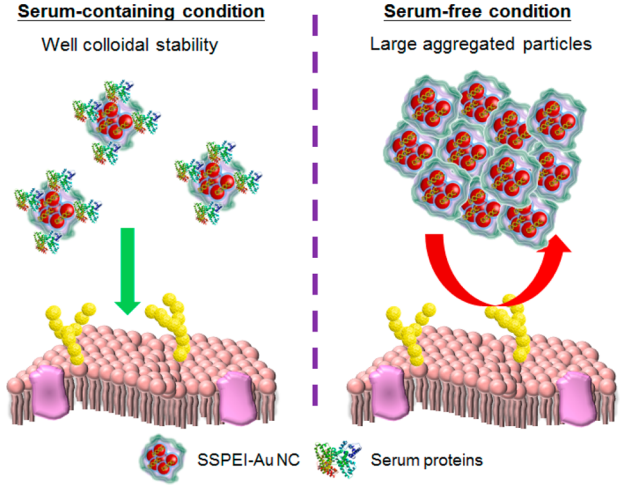

delivery. Interestingly, transfection efficiency of SSPEI-Au NC prepared by LBL assembly seems to be less affected by the presence of serum proteins. It was also noticed that the aggregation tendency of SSPEI-Au NC was minimized under a serum-containing environment compared to the serum-free condition. Thus, we speculated that enhanced colloidal stability may contribute to better cellular uptake and greater transgene expression of SSPEI-Au NC.

Effect of Serum on the Colloidal Stability of SSPEI-Au Nanocomplexes. The effect of serum proteins on the colloidal stability of SSPEI-Au NC was examined using a UV−vis spectroscopy. The SSPEI-Au NC formulated at various N/P ratios (43, 65, and 86) were incubated in the designated serum-containing mediums for 10 min or 8 h before acquiring the UV−vis spectra (Figure 9A). For 10 min incubation in serum-free medium, SSPEI-Au NC showed a high tendency of aggregation as evidenced by the SPR red shift of gold nanoparticles. With an extended incubation time (8 h), the UV−vis absorption of SSPEI-Au NC decreased to nearly background level and the solution became colorless due to the precipitation of aggregated SSPEI-Au NC (Figure 9B). In contrast, SSPEI-Au NC in the serum-containing mediums maintained good colloidal stability. The results suggest that serum proteins could assist the colloidal stability of SSPEI-Au NC. It is likely that serum proteins could adsorb onto the surface of SSPEI-Au NC via electrostatic or hydrophobic interactions to form a hydrophilic protein corona on SSPEI-Au NC for improved stability and greater transfection performance (Scheme 2).

CONCLUSIONS

To summarize, SSPEI-Au NC were successfully fabricated by LBL method and characterized for the physicochemical properties. SSPEI-Au NC exhibited efficient cellular uptake and low cytotoxicity. Interestedly, we observed that SSPEI-Au NC, in contrast to conventional cationic polymer-based gene delivery system, could maintain its transfection capability under serum-containing environment. This phenomenon might be attributed to the serum-assisted colloidal stability or enhanced cellular uptake of the SSPEI-Au NC under serum-containing condition. Current results suggest SSPEI-Au NC possesses great potential and is worth further evaluation as a new gene delivery tool.

ASSOCIATED CONTENT

Supporting Information

Figures S1−S4, which represent the results obtained for SSPEI-mediated transfection, cytotoxicity of SSPEI, effect of MUA or

DOI: 10.1021/acsami.5b00732
ACS Appl. Mater. Interfaces 2015, 7, 7724−7731

SSPEI coating concentration on the size/surface potential of SSPEI-Au NC/pDNA nanocomplexes, and effect of MUA or SSPEI coating concentration on the pDNA condensing ability of SSPEI-Au NC. This material is available free of charge via the Internet at http://pubs.acs.org.

AUTHOR INFORMATION

Corresponding Author

*E-mail: chienwen@mx.nthu.edu.tw. Tel.: 886-3-5715131, ext. 35531. Fax: 886-3-5718649.

Author Contributions

C.C.C. contributed to experiment design, acquisition of data, analysis and interpretation of data, and drafting of manuscript. C.W.C. contributed to the study conception and design, interpretation of data, and critical revision of the manuscript.

Notes

The authors declare no competing financial interest.

ACKNOWLEDGMENTS

This work was supported by grants from Ministry of Science and Technology of Taiwan (NSC102-2113-M-007-006-MY2), National Health Research Institutes (NHRI) of Taiwan (NHRI-EX103-10221EC), and National Tsing Hua University (104N2046E1). The authors are grateful to Mrs. Shang-Fang Chang for excellent technical assistance with transmission electron microscopy and Mr. Yen-Chun Lin with thermal analyzer, Instrumentation Center, National Tsing Hua University, Hsinchu, Taiwan.

REFERENCES

(1) Won, Y. W.; Adhikary, P. P.; Lim, K. S.; Kim, H. J.; Kim, J. K.; Kim, Y. H. Oligopeptide Complex for Targeted Non-Viral Gene Delivery to Adipocytes. *Nat. Mater.* **2014**, *13*, 1157−1164.

(2) Singha, K.; Namgung, R.; Kim, W. J. Polymers in Small-Interfering RNA Delivery. *Nucleic Acid Ther.* **2011**, *21*, 133−147.

(3) Kim, H. A.; Nam, K.; Kim, S. W. Tumor targeting RGD Conjugated Bio-reducible Polymer for VEGF siRNA Expressing Plasmid Delivery. *Biomaterials* **2014**, *35*, 7543−7552.

(4) Lee, Y. S.; Kim, S. W. Bioreducible Polymers for Therapeutic Gene Delivery. *J. Controlled Release* **2014**, *190*, 424−439.

(5) Wang, Y. H.; Zheng, M.; Meng, F. H.; Zhang, J.; Peng, R.; Zhong, Z. Y. Branched Polyethylenimine Derivatives with Reductively Cleavable Periphery for Safe and Efficient In Vitro Gene Transfer. *Biomacromolecules* **2011**, *12*, 1032−1040.

(6) Pouton, C. W.; Seymour, L. W. Key Issues in Non-viral Gene Delivery. *Adv. Drug Delivery Rev.* **2001**, *46*, 187−203.

(7) Zelphati, O.; Uyechi, L. S.; Barron, L. G.; Szoka, F. C., Jr. Effect of Serum Components on the Physico-Chemical Properties of Cationic Lipid/oligonucleotide Complexes and on their Interactions with Cells. *Biochim. Biophys. Acta* **1998**, *1390*, 119−133.

(8) Verbaan, F.; van Dam, I.; Takakura, Y.; Hashida, M.; Hennink, W.; Storm, G.; Oussoren, C. Intravenous Fate of poly(2-(dimethylamino)ethyl methacrylate)-Based Polyplexes. *Eur. J. Pharm. Sci.* **2003**, *20*, 419−427.

(9) Li, S.; Tseng, W. C.; Stolz, D. B.; Wu, S. P.; Watkins, S. C.; Huang, L. Dynamic Changes in the Characteristics of Cationic Lipidic Vectors after Exposure to Mouse Serum: Implications for Intravenous Lipofection. *Gene Ther.* **1999**, *6*, 585−594.

(10) Zhang, X. F.; Tang, W. X.; Yang, Z.; Luo, X. G.; Luo, H. Y.; Gao, D.; Chen, Y.; Jiang, Q.; Liu, J.; Jiang, Z. Z. PEGylated poly(amine-co-ester) Micelles as Biodegradable Non-viral Gene Vectors with Enhanced Stability, Reduced Toxicity and Higher In Vivo Transfection Efficacy. *J. Mater. Chem. B* **2014**, *2*, 4034−4044.

(11) Yang, F.; Green, J. J.; Dinio, T.; Keung, L.; Cho, S. W.; Park, H.; Langer, R.; Anderson, D. G. Gene Delivery to Human Adult and Embryonic Cell-Derived Stem Cells Using Biodegradable Nanoparticulate Polymeric Vectors. *Gene Ther.* **2009**, *16*, 533−546.

(12) Trubetskoy, V. S.; Wong, S. C.; Subbotin, V.; Budker, V. G.; Loomis, A.; Hagstrom, J. E.; Wolff, J. A. Recharging Cationic DNA Complexes with Highly Charged Polyanions for In Vitro and In Vivo Gene Delivery. *Gene Ther.* **2003**, *10*, 261−271.

(13) Li, P.; Liu, D. H.; Miao, L.; Liu, C. X.; Sun, X. L.; Liu, Y. J.; Zhang, N. A pH-sensitive Multifunctional Gene Carrier Assembled via Layer-By-Layer Technique for Efficient Gene Delivery. *Int. J. Nanomed.* **2012**, *7*, 925−939.

(14) Poon, Z.; Lee, J. B.; Morton, S. W.; Hammond, P. T. Controlling in Vivo Stability and Biodistribution in Electrostatically Assembled Nanoparticles for Systemic Delivery. *Nano Lett.* **2011**, *11*, 2096−2103.

(15) Li, L.; Jiang, W.; Luo, K.; Song, H. M.; Lan, F.; Wu, Y.; Gu, Z. W. Superparamagnetic Iron Oxide Nanoparticles as MRI Contrast Agents for Non-invasive Stem Cell Labeling and Tracking. *Theranostics* **2013**, *3*, 595−615.

(16) Huang, X. H.; Jain, P. K.; El-Sayed, I. H.; El-Sayed, M. A. Plasmonic Photothermal Therapy (PPTT) Using Gold Nanoparticles. *Laser Med. Sci.* **2008**, *23*, 217−228.

(17) Chiang, W. H.; Huang, W. C.; Chang, C. W.; Shen, M. Y.; Shih, Z. F.; Huang, Y. F.; Lin, S. C.; Chiu, H. C. Functionalized Polymersomes with Outlayered Polyelectrolyte Gels for Potential Tumor-Targeted Delivery of Multimodal Therapies and MR Imaging. *J. Controlled Release* **2013**, *168*, 280−288.

(18) Pissuwan, D.; Niidome, T.; Cortie, M. B. The Forthcoming Applications of Gold Nanoparticles in Drug and Gene Delivery Systems. *J. Controlled Release* **2011**, *149*, 65−71.

(19) Kumar, A.; Zhang, X.; Liang, X. J. Gold Nanoparticles: Emerging Paradigm for Targeted Drug Delivery System. *Biotechnol. Adv.* **2013**, *31*, 593−606.

(20) Poon, L.; Zandberg, W.; Hsiao, D.; Erno, Z.; Sen, D.; Gates, B. D.; Branda, N. R. Photothermal Release of Single-Stranded DNA from the Surface of Gold Nanoparticles Through Controlled Denaturating and Au-S Bond Breaking. *ACS Nano* **2010**, *4*, 6395−6403.

(21) Zhang, W. Q.; Meng, J.; Ji, Y. L.; Li, X. J.; Kong, H.; Wu, X. C.; Xu, H. Y. Inhibiting Metastasis of Breast Cancer Cells In Vitro Using Gold Nanorod-siRNA Delivery System. *Nanoscale* **2011**, *3*, 3923−3932.

(22) Conde, J.; Ambrosone, A.; Sanz, V.; Hernandez, Y.; Marchesano, V.; Tian, F. R.; Child, H.; Berry, C. C.; Ibarra, M. R.; Baptista, P. V.; Tortiglione, C.; de la Fuente, J. M. Design of Multifunctional Gold Nanoparticles for In Vitro and In Vivo Gene Silencing. *ACS Nano* **2012**, *6*, 8316−8324.

(23) Timko, B. P.; Dvir, T.; Kohane, D. S. Remotely Triggerable Drug Delivery Systems. *Adv. Mater.* **2010**, *22*, 4925−4943.

(24) Figueroa, E. R.; Lin, A. Y.; Yan, J. X.; Luo, L.; Foster, A. E.; Drezek, R. A. Optimization of PAMAM-Gold Nanoparticle Conjugation for Gene Therapy. *Biomaterials* **2014**, *35*, 1725−1734.

(25) Tencomnao, T.; Apijaraskul, A.; Rakkhithawatthana, V.; Chaleawlert-umpon, S.; Pimpa, N.; Sajomsang, W.; Saengkrit, N. Gold/cationic Polymer Nano-Scaffolds Mediated Transfection for Non-viral Gene Delivery System. *Carbohydr. Polym.* **2011**, *84*, 216−222.

(26) Xia, W.; Wang, P.; Lin, C.; Li, Z.; Gao, X.; Wang, G.; Zhao, X. Bioreducible Polyethylenimine-Delivered siRNA Targeting Human Telomerase Reverse Transcriptase Inhibits HepG2 Cell Growth In Vitro and In Vivo. *J. Controlled Release* **2012**, *157*, 427−436.

(27) Christensen, L. V.; Chang, C. W.; Kim, W. J.; Kim, S. W.; Zhong, Z. Y.; Lin, C.; Engbersen, J. F. J.; Feijen, J. Reducible poly(amido ethylenimine)s Designed for Triggered Intracellular Gene Delivery. *Bioconjugate Chem.* **2006**, *17*, 1233−1240.

(28) Dorris, A.; Rucareanu, S.; Reven, L.; Barrett, C. J.; Lennox, R. B. Preparation and Characterization of Polyelectrolyte-Coated Gold Nanoparticles. *Langmuir* **2008**, *24*, 2532−2538.

(29) Shih, I. L.; Van, Y. T. The Production of poly-(gamma-glutamic acid) from Microorganisms and its Various Applications. *Bioresour. Technol.* **2001**, *79*, 207−225.

DOI: 10.1021/acsami.5b00732
ACS Appl. Mater. Interfaces 2015, 7, 7724−7731

(30) Lin, Y. H.; Chen, C. T.; Liang, H. F.; Kulkarni, A. R.; Lee, P. W.; Chen, C. H.; Sung, H. W. Novel Nanoparticles for Oral Insulin Delivery via the Paracellular Pathway. *Nanotechnology* **2007**, *18*, 105102−105112.
(31) Kurosaki, T.; Kitahara, T.; Fumoto, S.; Nishida, K.; Nakamura, J.; Niidome, T.; Kodama, Y.; Nakagawa, H.; To, H.; Sasaki, H. Ternary Complexes of pDNA, polyethylenimine, and Gamma-polyglutamic Acid for Gene Delivery Systems. *Biomaterials* **2009**, *30*, 2846−2853.

DOI: 10.1021/acsami.5b00732
ACS Appl. Mater. Interfaces 2015, 7, 7724−7731